dFezf/Earmuff Maintains the Restricted Developmental Potential of Intermediate Neural Progenitors in *Drosophila*

Mo Weng,[1,2] Krista L. Golden,[2] and Cheng-Yu Lee[1,2,3,*]
[1]Department of Cell and Developmental Biology, University of Michigan Medical School, Ann Arbor, MI, USA
[2]Center For Stem Cell Biology, Life Sciences Institute, University of Michigan, Ann Arbor, MI 48109, USA
[3]Division of Molecular Medicine and Genetics, Department of Internal Medicine, University of Michigan Medical School, Ann Arbor, MI, USA
*Correspondence: leecheng@umich.edu
DOI 10.1016/j.devcel.2009.12.007

SUMMARY

To ensure normal development and maintenance of homeostasis, the extensive developmental potential of stem cells must be functionally distinguished from the limited developmental potential of transit amplifying cells. Yet the mechanisms that restrict the developmental potential of transit amplifying cells are poorly understood. Here we show that the evolutionarily conserved transcription factor dFezf/ Earmuff (Erm) functions cell-autonomously to maintain the restricted developmental potential of the intermediate neural progenitors generated by type II neuroblasts in *Drosophila* larval brains. Although *erm* mutant intermediate neural progenitors are correctly specified and show normal apical-basal cortical polarity, they can dedifferentiate back into a neuroblast state, functionally indistinguishable from normal type II neuroblasts. Erm restricts the potential of intermediate neural progenitors by activating Prospero to limit proliferation and by antagonizing Notch signaling to prevent dedifferentiation. We conclude that Erm dependence functionally distinguishes intermediate neural progenitors from neuroblasts in the *Drosophila* larval brain, balancing neurogenesis with stem cell maintenance.

INTRODUCTION

Tissue development and homeostasis often require stem cells to transiently expand the progenitor pool by producing transit amplifying cells. Yet the developmental potential of transit amplifying cells must be tightly restricted to ensure generation of differentiated progeny and to prevent unrestrained proliferation that might lead to tumorigenesis (Morrison and Kimble, 2006; Pontious et al., 2008; Vescovi et al., 2006). Transit amplifying cells are defined by their limited developmental capacity, a feature specified during fate determination (Farkas et al., 2008; Hodge et al., 2008; Sessa et al., 2008). It is unknown whether an active mechanism is required to maintain restricted developmental potential in transit amplifying cells after specification. Here we use *i*ntermediate *n*eural *p*rogenitors (INPs) in

developing *Drosophila* larval brains as a genetic model to investigate how restricted developmental potential is regulated in transit amplifying cells.

A fly larval brain hemisphere contains eight type II neuroblasts that undergo repeated asymmetric divisions to self-renew and to generate immature INPs (Figure 1A) (Bello et al., 2008; Boone and Doe, 2008; Bowman et al., 2008). Immature INPs are unstable in nature and are mitotically inactive, and they lack the expression of Deadpan (Dpn) and Asense (Ase) (Figure S1A). Immature INPs commit to the INP fate through maturation, a differentiation process necessary for specification of the INP identity (Figure 1A). INPs express Dpn and Ase, and undergo 8–10 rounds of asymmetric divisions to self-renew and to produce ganglion mother cells (GMCs) that typically generate two neurons (Figure S1A) (Bello et al., 2008; Boone and Doe, 2008; Bowman et al., 2008). While 5–6 immature INPs and 1–2 young INPs are always in direct contact with their parental neuroblasts, the older INPs become progressively displaced from their parental neuroblasts over time (Bowman et al., 2008).

During asymmetric divisions of type II neuroblasts, the basal proteins Brain tumor and Numb are exclusively segregated into immature INPs, and function cooperatively, but nonredundantly, to ensure that immature INPs undergo maturation and commit to the INP fate (Boone and Doe, 2008; Bowman et al., 2008). *brain tumor* or *numb* mutant type II neuroblasts generate immature INPs that fail to mature and do not commit to the INP fate. Instead, *brain tumor* or *numb* mutant immature INPs adopt their parental neuroblast fate, leading to supernumerary type II neuroblasts. Thus, *brain tumor* and *numb* specify the INP fate, and the ectopic expansion of type II neuroblasts in these mutant genetic backgrounds occurs due to failure to properly specify the INP fate. Although Brain tumor is also asymmetrically segregated into GMCs during asymmetric divisions of INPs, the mosaic clones in *brain tumor* mutant INPs contain only differentiated neurons (Bowman et al., 2008). This result indicates that Brain tumor is dispensable for maintaining the restricted developmental potential of INPs. How restricted developmental potential is maintained in INPs is currently unknown.

To identify genes that regulate self-renewal of neuroblasts, we conducted a genetic screen for mutants exhibiting ectopic larval brain neuroblasts (C.-Y.L. and C.Q. Doe, unpublished data). One mutation, *l(2)5138*, specifically resulted in massive expansion of neuroblasts in the brain but did not affect neuroblasts on the
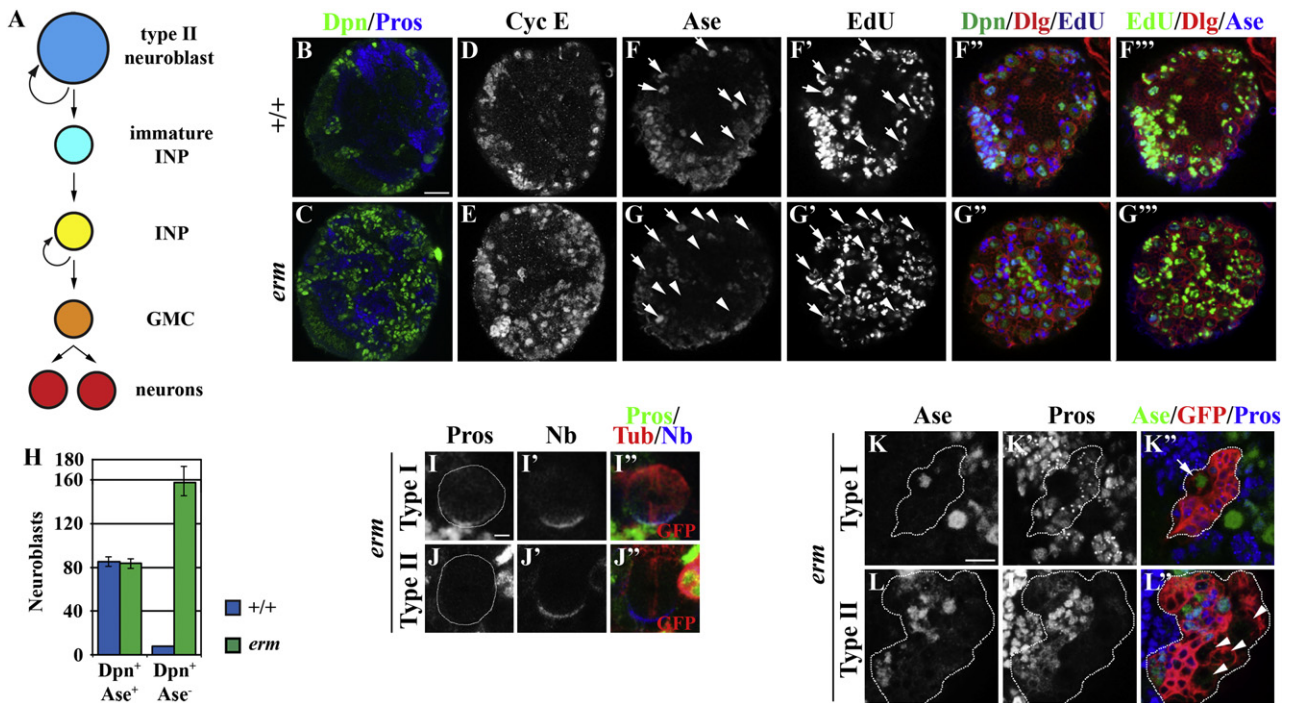
Figure 1. *erm* Mutant Brains Show Ectopic Type II Neuroblasts

(A) A summary of the type II neuroblast lineage.

(B–H) While wild-type (+/+) and *erm* mutant brains contained a similar number of type I neuroblasts (Dpn$^+$CycE$^+$Ase$^+$EdU$^+$; white arrows), *erm* mutant brains contained ectopic type II neuroblasts (Dpn$^+$CycE$^+$Ase$^-$EdU$^+$; white arrowheads). In (H), wild-type brains contained 85 ± 5.2 type I neuroblasts and 8.0 ± 0 type II neuroblasts, whereas *erm* mutant brains contained 83.7 ± 6.4 type I neruoblasts and 159 ± 19.7 type II neuroblasts. Scale bar, 20 μm.

(I and J) In *erm* mutant brains expressing GFP driven by *Ase-Gal4*, Prospero (Pros) always colocalized with Numb (Nb) in metaphase type I neuroblasts (GFP$^+$; white circle), but never in type II neuroblasts (GFP$^-$; white circle). Scale bar, 2 μm.

(K and L) *erm* mutant type I neuroblast clones (white circle) always contained a single neuroblast (white arrow), but *erm* mutant type II neuroblast clones (white circle) always contained multiple neuroblasts (white arrowheads).

ventral nerve cord (Figures S1B–S1D). We mapped the *l(2)5138* mutation to the 22B4-7 chromosomal interval that contains the *earmuff* (*erm*) gene (Pfeiffer et al., 2008). The *erm* transcripts are first detected at embryonic stage 4–6 in the specific domain preceding formation of the embryonic brain and remain highly expressed in the brain throughout development (Chintapalli et al., 2007; Pfeiffer et al., 2008). Here, we report that Erm functions to restrict the developmental potential of INPs by promoting Prospero-dependent termination of proliferation and suppressing Notch-mediated dedifferentiation. By restricting their developmental potential, Erm ensures that INPs generate only differentiated neurons during *Drosophila* neurogenesis.

RESULTS

Earmuff Prevents Abnormal Expansion of Neural Progenitors in Type II Neuroblast Lineages

All neuroblasts in *l(2)5138* homozygous mutant brains were proliferative, expressed all known neuroblast markers, and lacked neuronal and glial markers (Figures 1B–1G; Figures S1B–S1D; data not shown). We mapped the *l(2)5138* mutation to the *erm* gene, which encodes a homolog of the vertebrate *F*orebrain *e*mbryonic *z*inc-*f*inger family (Fezf) transcription factors (Hashimoto et al., 2000; Matsuo-Takasaki et al., 2000). The *l(2)5138* mutants contained a single A→T nucleotide change

in the *erm* coding region, leading to the substitution of a leucine for a conserved histidine in the third C$_2$H$_2$ zinc-finger domain (data not shown). Consistent with its predicted molecular function, ectopic expression of Erm transgenic proteins tagged with a HA epitope at the amino- or carboxyl-terminus driven by neuroblast-specific *Wor-Gal4* was detected in the nuclei of neuroblasts (data not shown). However, the expression of the HA-tagged Erm transgenic protein bearing the identical leucine-to-histidine substitution as in the *l(2)5138* mutant was undetectable, suggesting that the mutant Erm protein is unstable (data not presented). We conclude that *l(2)5138* is a mutant allele of *erm*.

To determine whether *erm* mutant brains have ectopic type I and/or type II neuroblasts, we analyzed the expression pattern of Ase and Prospero (Pros), which are only expressed in type I neuroblasts (Figure S1A) (Bello et al., 2008; Boone and Doe, 2008; Bowman et al., 2008). We found that *erm* mutant brains contained over 20-fold more type II neuroblasts (Dpn$^+$Ase$^-$) than wild-type brains, with no significant change in the number of type I neuroblasts (Dpn$^+$Ase$^+$) (Figures 1F–1H). Next, we analyzed the localization of Prospero in mitotic neuroblasts in larval brains expressing GFP induced by *Ase-Gal4* (*Ase > GFP*), which mimicked the expression pattern of the endogenous Ase protein (Bowman et al., 2008). In *erm* mutant larval brains, all mitotic type I neuroblasts (GFP$^+$) showed formation of basal Prospero crescents, but none of the mitotic type II neuroblasts
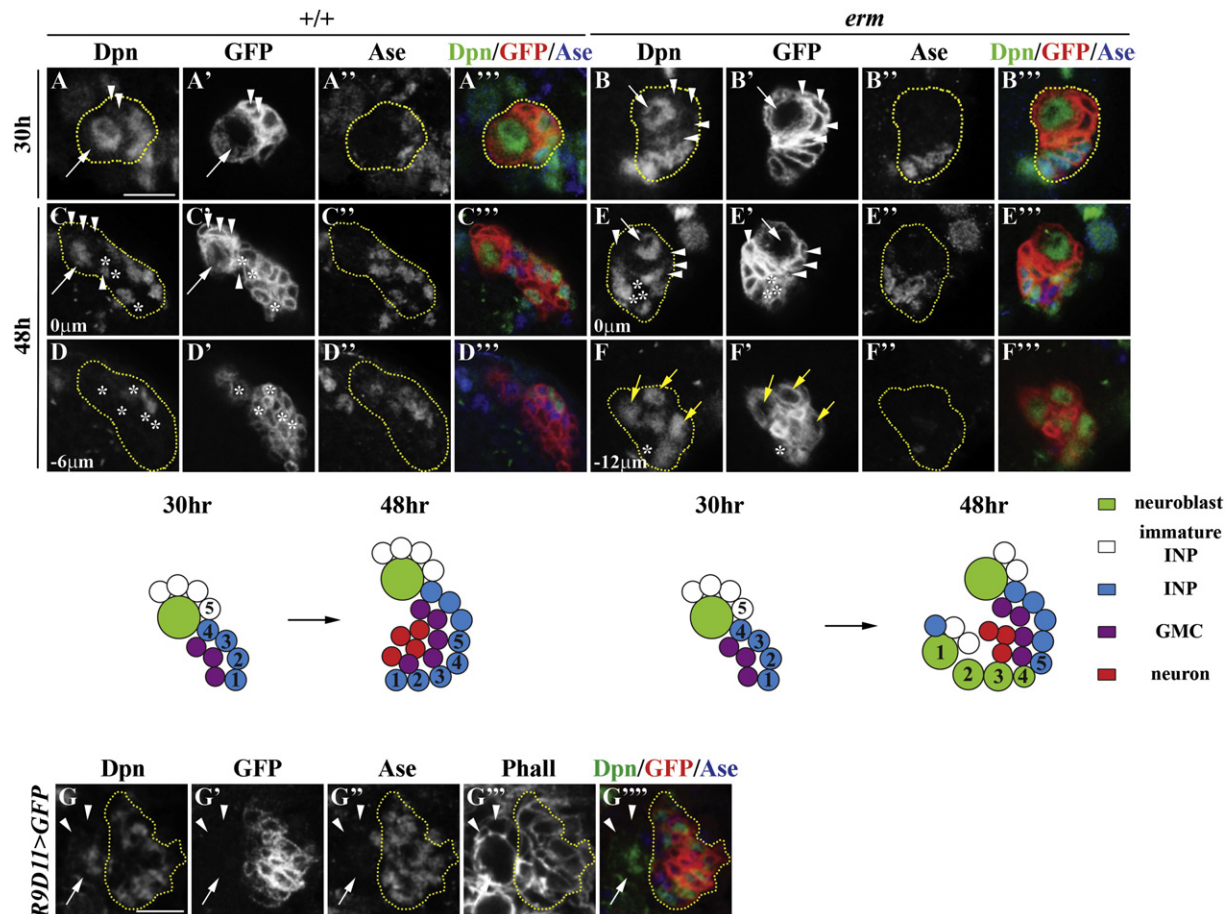
Figure 2. Erm Maintains the Limited Developmental Potential of INPs

(A and B) At 30 hr after clone induction, both wild-type (+/+) and *erm* mutant neuroblast clones (yellow circles) contained a single parental neuroblast (white arrows) directly surrounded by immature INPs (white arrowheads) and 1–2 young INPs (Dpn$^+$Ase$^+$).

(C–F) At 48 hr after clone induction, wild-type (+/+) neuroblast clones (yellow circles) contained a single parental neuroblast (white arrows) in direct contact with immature INPs (white arrowheads) and young INPs (Dpn$^+$Ase$^+$). Older INPs were away from their parental neuroblasts and were surrounded by GMCs (white asterisks) and neurons (Dpn$^-$Ase$^-$). In contrast, the *erm* mutant clones contained ectopic type II neuroblast-like cells ([F], yellow arrows) further from the parental neuroblasts than most INPs and neurons. A summary diagram is shown below.

(G) *R9D11-Gal4* (*Erm-Gal4*) was undetectable in type II neuroblasts (white arrow) and immature INPs (white arrowheads), but was clearly detected in INPs. All scale bars, 10 μm.

(GFP$^-$) showed the expression of Prospero (Figures 1I and 1J; n = 20). Furthermore, GFP-marked *erm* mutant type II neuroblast clones consistently contained multiple type II neuroblasts, whereas *erm* mutant type I neuroblast clones always contained single type I neuroblasts and neurons (Figures 1K and 1L). We conclude that *erm* mutant brains exhibit an abnormal expansion of type II neuroblasts.

erm Regulates the Developmental Potential of INPs

To determine the cellular origin of ectopic type II neuroblasts in *erm* mutant brains, we analyzed the identity of cells in the GFP-marked clones derived from wild-type or *erm* mutant type II neuroblasts using specific cell fate markers. At 30 hr after clone induction, wild-type and *erm* mutant neuroblast clones appeared indistinguishable, containing single parental neuroblasts (Dpn$^+$Ase$^-$; ≥10 μm) in direct contact with 5–6 immature INPs (Dpn$^-$Ase$^-$), while most of the INPs (Dpn$^+$Ase$^+$; ≥6 μm) were 1

cell or more away from the parental neuroblasts (Figures 2A and 2B). At 48 hr after clone induction, the overall size of both wild-type and *erm* mutant neuroblast clones increased significantly due to an increase in cell number, reflecting continuous asymmetric divisions of the parental neuroblasts. In both wild-type and *erm* mutant clones, the parental neuroblasts remained surrounded by 5–6 immature INPs, while INPs and differentiated neurons (Dpn$^-$Ase$^-$Pros$^+$) were found several cells away from the parental neuroblasts (Figures 2C–2F; Figures S2A–S2F). However, *erm* mutant clones contained fewer INPs (16 ± 4; n = 10 brains) than the wild-type clones (21 ± 4; n = 10 brains). Importantly, *erm* mutant clones consistently contained 4–6 smaller ectopic type II neuroblasts (Dpn$^+$Ase$^-$; 6–8 μm in diameter) (Figure 2F; Figure S2F). Thus, Erm is dispensable for both the generation and maturation of immature INPs.

Ectopic type II neuroblasts in 48 hr *erm* mutant clones were always several cells away from the parental neuroblasts
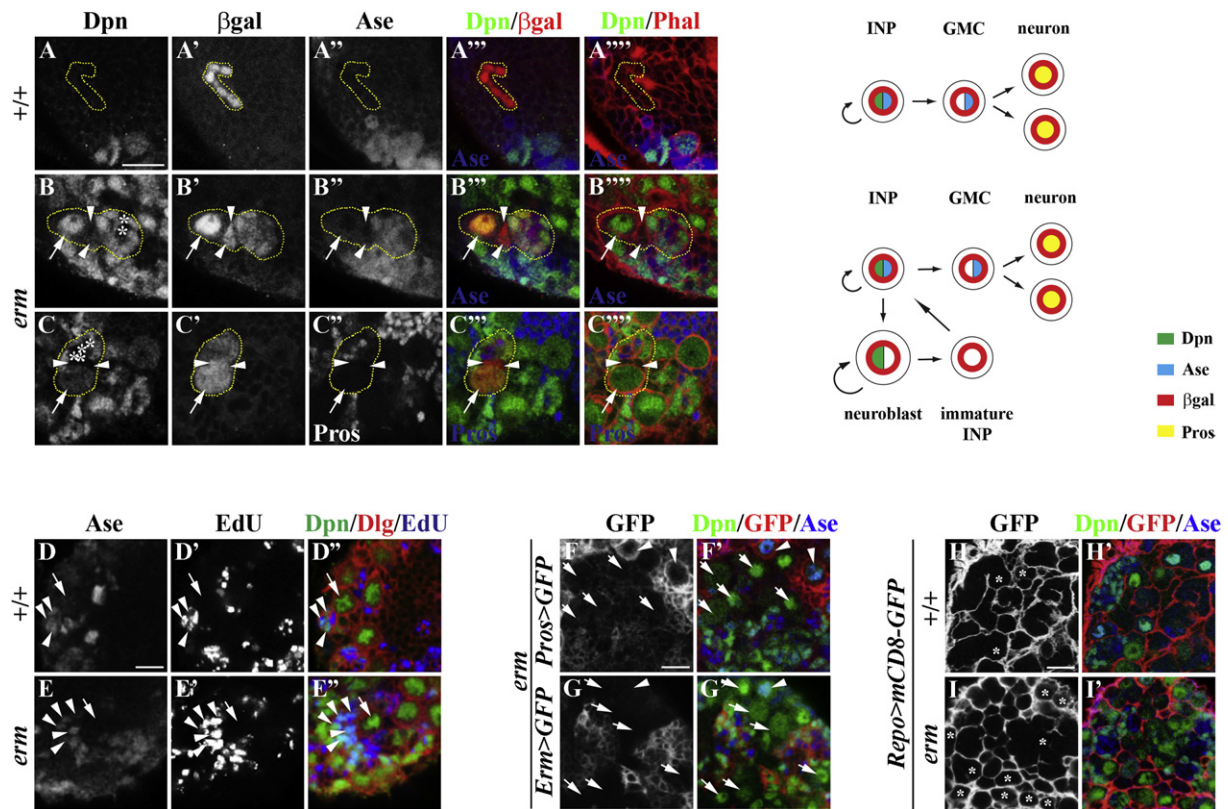
Figure 3. *erm* Suppresses the Dedifferentiation of INPs

(A–C) A wild-type (+/+) INP only generated neurons (Dpn⁻Ase⁻), but an *erm* mutant INP generated dedifferentiated neuroblasts (white arrows), immature INPs (white arrowheads) and INPs (Dpn⁺Ase⁺), GMCs ([B], white asterisks), and neurons ([C], white asterisks). A lineage clone is circled in yellow, and a summary diagram is shown on the right.

(D–I) Similar to wild-type type II neuroblasts, ectopic type II neuroblasts in *erm* mutant brains lost incorporated EdU (neuroblasts, white arrows; INPs, white arrowheads) (D and E), did not express *Pros-Gal4* and *Erm-Gal4* (type I neuroblast, white arrowheads; type II neuroblasts, white arrows) (F and G), and established ectopic neuroblast lineages (white asterisks) surrounded by glial membrane (H and I). All scale bars, 10 μm.

(Figure 2F; Figure S2F). This result strongly suggests that ectopic type II neuroblasts in *erm* mutant clones likely originate from INPs and Erm likely functions in INPs. However, we could not assess the spatial expression pattern of the endogenous Erm protein in larval brains due to lack of a specific antibody and low signals by fluorescent RNA in situ (data not shown). Alternatively, we analyzed the expression of the *R9D* series of *Gal4* transgenes in which Gal4 is expressed under the control of overlapping *erm* promoter fragments (Pfeiffer et al., 2008). The expression of *R9D11-Gal4* was clearly detected in INPs, but was undetectable in type II neuroblasts and immature INPs even when two copies of the *UAS-mCD8-GFP* transgenes were driven by two copies of *R9D11-Gal4* at 32°C for 72 hr after larval hatching (Figure 2G; Figure S2G). Consistently, the expression of *Erm-Gal4* was virtually undetectable in *brain tumor* mutant brains that contain thousands of type II neuroblasts and immature INPs (Figure S2H). While the expression of *UAS-erm* induced by the neuroblast-specific *Wor-Gal4* driver led to premature loss of type II neuroblasts, expression of *UAS-erm* driven by *Erm-Gal4* failed to exert any effect on type II neuroblasts (data not shown). Importantly, targeted expression of the fly Erm or mouse Fezf1 or Fezf2 transgenic protein driven

by *R9D11-Gal4* restored the function of Erm and efficiently rescued the ectopic neuroblast phenotype in *erm* mutant brains (Figures S2I–S2L). Therefore, *R9D11-Gal4* (*Erm-Gal4*) contains the enhancer element sufficient to restore the Erm function in INPs leading to suppression of ectopic type II neuroblasts in *erm* mutant brains.

erm Mutant INPs Dedifferentiate Back into Type II Neuroblasts

Mutant clonal analyses and overexpression studies strongly suggest that Erm functions to suppress reversion of INPs back into a neuroblast state. Here, we directly tested whether INPs in *erm* mutant brains can dedifferentiate back into type II neuroblasts. We induced βgal-marked lineage clones originating exclusively from INPs via FRT-mediated recombination. We targeted a short pulse of flipase (FLP) expression in INPs by heat-shocking larvae carrying a *UAS-flp* transgene under the control of *Erm-Gal4* and *tub-Gal80ts* at 30°C for 1 hr (see Experimental Procedures for details). At 72 hr after heat shock, INP clones in wild-type brains contained only differentiated neurons (Dpn⁻Ase⁻) (Figure 3A). In contrast, INP clones in *erm* mutant brains contained one or more type II neuroblasts as well as immature

INPs, INPs, GMCs, and neurons (Figures 3B–3C). This result indicates that while INPs in wild-type larval brains can only give rise to neurons, INPs in *erm* mutant brains can dedifferentiate into type II neuroblasts that can give rise to all cell types found in a normal type II neuroblast lineage. We conclude that Erm functions to maintain the restricted developmental potential of INPs and prevents them from dedifferentiating back into a neuroblast state.

We further assessed whether the dedifferentiated type II neuroblasts in *erm* mutant brains displayed multiple functional characteristics of normal type II neuroblasts.

Apical-Basal Cell Polarity

All mitotic type II neuroblasts in wild-type and *erm* mutant brains showed normal establishment and maintenance of cortical polarity by asymmetrically localizing and segregating atypical Protein Kinase C (aPKC), Pins, Miranda, and Numb (data not shown).

Proliferation Profile

All wild-type and *erm* mutant type II neuroblasts could be labeled with a 3 hr pulse of the thymidine analog EdU (Figures 1F′ and 1FG′), and incorporated EdU can be chased into INPs following a 12 hr EdU-free chase (Figures 3D and 3E).

prospero and earmuff Promoter Activity

While all type I neuroblasts in wild-type and *erm* mutant brains expressed *Pros-Gal4* but lacked *Erm-Gal4* expression, none of the type II neuroblasts in wild-type and *erm* mutant brains showed detectable expression of *Pros-Gal4* or *Erm-Gal4* (Figures 3F and 3G; data not shown).

Formation of Glial Chambers

Individual neuroblast lineages are surrounded by the cortex glial membrane forming distinct chambers (Pereanu et al., 2005). A wild-type brain hemisphere contained eight glial chambers encapsulating eight individual type II neuroblast lineages (Figure 3H). In contrast, an *erm* mutant brain hemisphere contained more than 50 glial chambers, each containing one or more type II neuroblasts and their presumptive progeny (Figure 3I).

Taken together, INPs in *erm* mutant brains dedifferentiate back into apparently normal neuroblasts that can establish ectopic type II neuroblast lineages.

erm Mutant INPs Exhibit Normal Apical-Basal Cortical Polarity

Dysregulation of apical-basal polarity can lead to failure in differentiation and result in ectopic neuroblasts at the expense of GMC formation (Betschinger et al., 2006; Lee et al., 2006a, 2006b, 2006c; Wang et al., 2006). To determine whether the dedifferentiation of INPs in *erm* mutant brains might be due to defects in cortical polarity, we assayed apical-basal polarity by examining the localization of aPKC, Miranda, Prospero, and Numb in larval brains expressing GFP driven by *Ase-GAL4* (*Ase > GFP*). Mitotic INPs (GFP⁺) in *erm* mutant brains showed the same asymmetric localization of aPKC, Miranda, Prospero, and Numb as in wild-type brains (Figures 4A and 4B; data not shown). Thus, we conclude that INPs in *erm* mutant brains dedifferentiate while displaying normal cortical polarity.

Erm Restricts Proliferation by Activating Prospero-Dependent Cell Cycle Exit

To determine how Erm maintains the restricted developmental potential of INPs, we performed microarray analyses and found
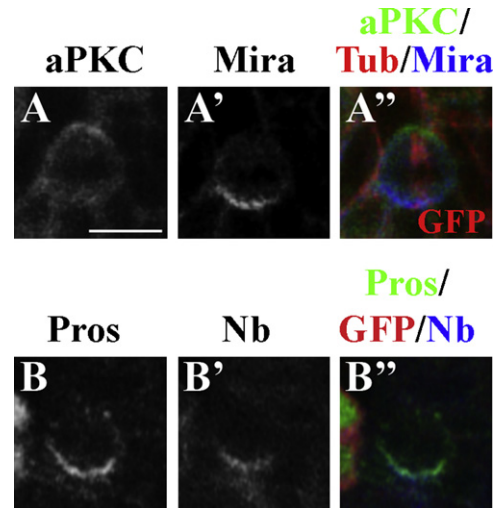

Figure 4. *erm* Mutant INPs Show Normal Apical-Basal Polarity
(A and B) Metaphase INPs in *erm* mutant brains expressing GFP induced by *Ase-Gal4* showed asymmetric localization of aPKC, Miranda (Mira), Pros, and Numb (Nb). The scale bar, 5 μm.

that *prospero* mRNA was drastically reduced in *erm* mutant brains compared to the control brains (M.W. and C.-Y.L., unpublished data). We confirmed that the relative level of *prospero* mRNA was indeed reduced by 60%–70% in *erm* mutant brain extracts by using real-time PCR (data not shown). These data supported that Erm is necessary for proper transcription of *prospero*, and prompted us to test if overexpression of Erm might be sufficient to induce ectopic Prospero expression. We induced a short pulse of Erm expression in brain neuroblasts by shifting larvae carrying a *UAS-erm* transgene under the control of *Wor-Gal4* and *tub-Gal80^{ts}* to from 25°C to 30°C. A 3.5 hr pulse of Erm expression was sufficient to induce nuclear localization of Prospero in larval brain neuroblasts (Figure 5A). Consistent with nuclear Prospero promoting termination of neuroblast proliferation, ectopic expression of Erm induced by *Wor-Gal4* resulted in decreased neuroblasts compared to wild-type brains (Figure 5B). Thus, we conclude that overexpression of Erm can restrict neuroblast proliferation by triggering nuclear localization of Pros.

Our data suggest that Erm might restrict the developmental potential of INPs in part by limiting their proliferation by activating Prospero-dependent cell cycle exit. If so, we predict that overexpression of Erm should induce ectopic nuclear Prospero in INPs and overexpression of Prospero should suppress ectopic neuroblasts in *erm* mutant brains. In wild-type brains, 9.6% of INPs (32/325) showed nuclear localization of Prospero. However, overexpression of Erm driven by *Erm-Gal4* led to nuclear localization of Prospero in 41.5% of INPs (105/253), likely restricting their proliferation potential and resulting in some parental type II neuroblasts surrounded only by differentiated neurons (Figures 5C and 5D). Importantly, ectopic expression of Prospero induced by *Erm-Gal4* efficiently suppressed ectopic neuroblasts and restored neuronal differentiation in *erm* mutant brains (Figures 5E and 5F). Thus, Erm likely restricts the proliferation of INPs by promoting nuclear localization of Prospero. To confirm that
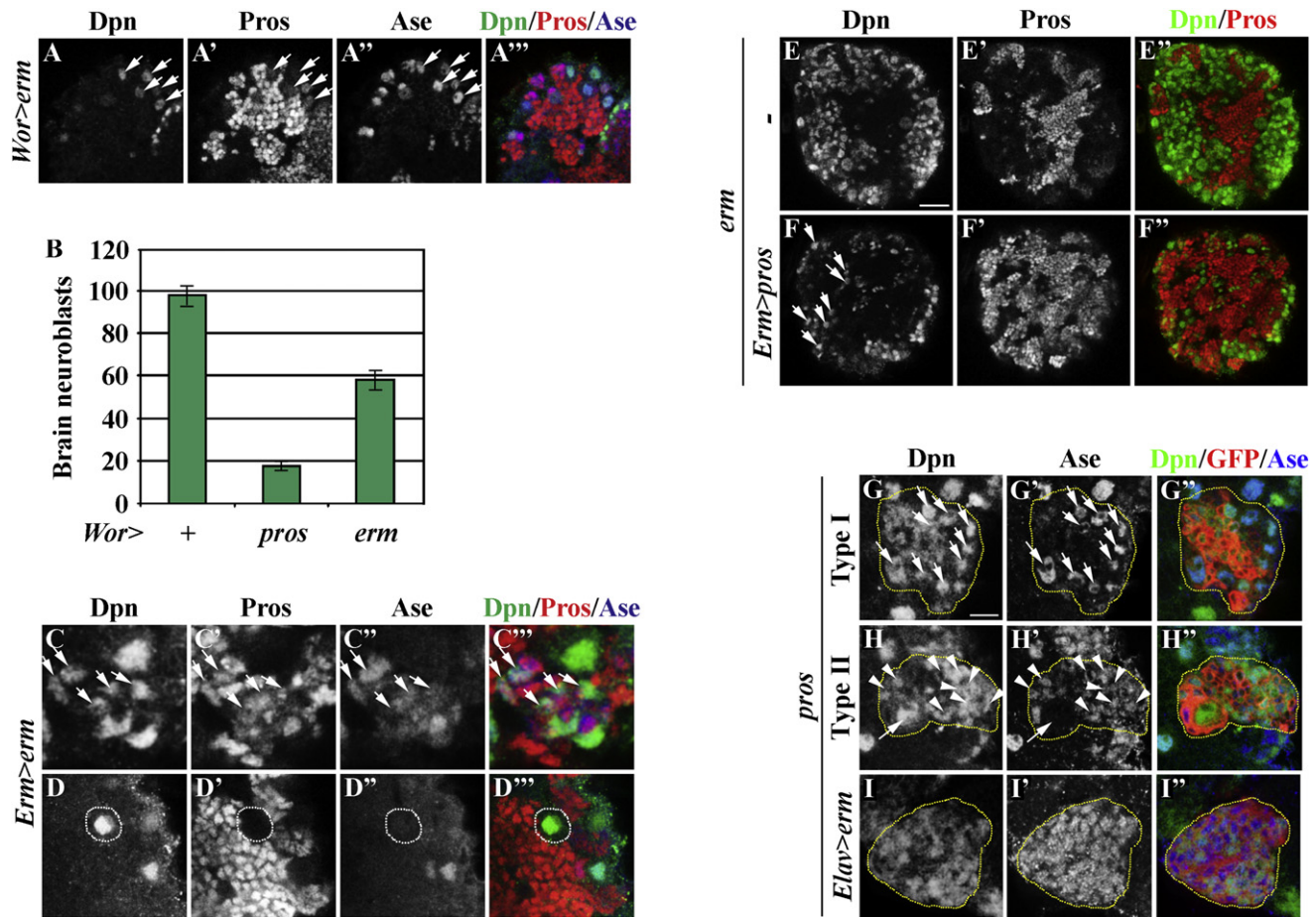
Figure 5. Erm Restricts the Proliferation of INPs by Promoting Nuclear Prospero

(A) A 3.5 hr pulse of Erm expression induced by *Wor-Gal4* was sufficient to trigger Pros localization in neuroblast nuclei (white arrows).

(B) Ectopic expression of Erm (57.9 ± 8.6) or Pros (17.4 ± 4.4 neuroblasts) driven by *Wor-Gal4* was sufficient to terminate neuroblast proliferation prematurely (98.0 ± 8.4 neuroblasts in wild-type brains).

(C and D) Ectopic expression of Erm induced by *Erm-Gal4* triggered a significant increased in INPs that exhibited nuclear Pros (white arrows), likely leading them to exit cell cycle prematurely and resulting in some type II neuroblasts (white circle) surrounded only by neurons. Scale bar, 10 μm.

(E and F) Overexpression of Pros induced by *Erm-Gal4* suppressed ectopic neuroblasts and restored neuronal differentiation in *erm* mutant brains. Scale bar, 20 μm.

(G and H) *pros* mutant type I neuroblast clones contained ectopic neuroblasts (white arrows). *pros* mutant type II neuroblast clones contained a single type II neuroblast (white arrow) but showed dramatic overproliferation of INPs (white arrowheads).

(I) Overexpression of Erm failed to suppress overproliferation of INPs in *pros* mutant type II neuroblast clones. Scale bar, 10 μm.

Prospero indeed functions downstream of Erm to restrict the proliferation of INPs, we performed genetic epistatic analyses. Consistent with previously published results, *prospero* mutant type I neuroblast clones contained ectopic type I neuroblasts (Figure 5G) (Bowman et al., 2008). In contrast, *prospero* mutant type II neuroblast clones exhibited accumulation of ectopic INPs while maintaining single parental neuroblasts (Figure 5H). Furthermore, overexpression of Erm failed to suppress ectopic INPs in *prospero* mutant type II neuroblast clones, consistent with Prospero functioning downstream of Erm (Figure 5I). These results indicate that blocking differentiation is not sufficient to trigger the dedifferentiation of INPs back into type II neuroblasts. Thus, Erm's restriction on the proliferation of INPs is dependent on Prospero function, but its suppression of the dedifferentiation of INPs is independent of Prospero.

Erm Suppresses Dedifferentiation by Antagonizing Notch Signaling

Previous studies showed that overexpression of constitutively active Notch (Notch[intra]) in both type I and II neuroblasts is sufficient to trigger ectopic neuroblasts (Bowman et al., 2008; Wang et al., 2006). Here, we tested whether Erm suppresses the dedifferentiation of INPs by inhibiting Notch signaling. Indeed, knockdown of Notch function by RNAi in *erm* mutant brains led to a dramatic reduction in ectopic type II neuroblasts compared to *erm* mutant brains alone (Figures 6A and 6B). Complementarily, ectopic expression of constitutively active Notch (Notch[intra]) induced by *Erm-Gal4* transforms INPs into ectopic type II neuroblasts (Figure 6C). Thus, reduced Notch function suppresses the dedifferentiation of INPs in *erm* mutant brains whereas ectopic activation of Notch induces the dedifferentiation of INPs. We
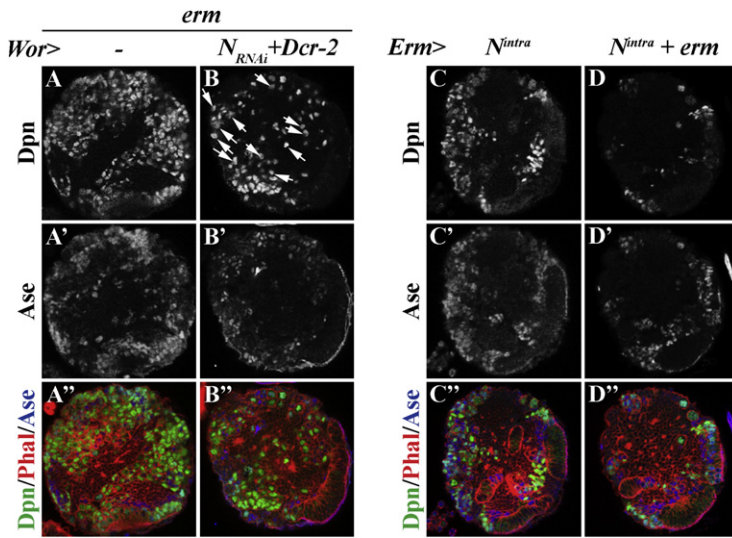
Figure 6. Erm Suppresses the Dedifferentiation of INPs by Negatively Regulating Notch Signaling

(A and B) Knocking down Notch function by RNAi suppressed ectopic neuroblasts (white arrows) in *erm* mutant brains.

(C and D) Ectopic expression of Erm under the control of *Erm-Gal4* suppressed ectopic neuroblasts induced by constitutive activation of Notch signaling. Scale bar, 20 μm.

next tested if Erm suppresses the dedifferentiation of INPs by antagonizing a Notch-activated mechanism. Coexpression of Erm under the control of *Erm-Gal4* is sufficient to suppress ectopic neuroblasts induced by the expression of Notch[intra] (Figure 6D). Thus, we conclude that Erm can suppress the dedifferentiation of INPs by negatively regulating a Notch-activated signaling mechanism.

DISCUSSION

The limited developmental potential of transit amplifying cells is generally thought to be specified during fate determination (Farkas et al., 2008; Hodge et al., 2008; Sessa et al., 2008). In this study, we report a mechanism that actively maintains the restricted developmental potential of transit amplifying cells after specification of their identity. We show that the evolutionarily conserved transcription factor Erm/Fezf functions to maintain the restricted developmental potential of INPs by limiting their proliferation potential and suppressing their dedifferentiation capacity (Figure 7). Combining proper specification of the transit amplifying cell identity and active maintenance of their restricted developmental potential ensures the generation of differentiated progeny and prevents aberrant expansion of stem cells.

The lineage clones derived from single INPs in *erm¹/erm²* mutant brains contain dedifferentiated neuroblasts, immature

INPs, INPs, GMCs, and neurons (Figures 3B and 3C). Several mechanisms could lead to the diversity of cells within the clones. First, INPs in *erm* mutant brains might generate GMCs and neurons initially due to the presence of maternally deposited Erm. However, *erm* transcripts are undetectable in both adult male and female germlines by microarray analyses and in stage 1–3 embryos by RNA in situ (Chintapalli et al., 2007; http://flybase.org/reports/FBgn0031375.html; data not shown). Furthermore, the *erm¹/erm²* allelic combination resulted in little to no zygotic Erm in the brain because the *erm¹* mutation likely leads to the production of an unstable Erm protein, whereas the *erm²* mutation deletes the entire *erm* open reading frame (data not shown). Additionally, the ectopic neuroblast phenotype in *erm¹/erm²* mutant brains can be observed as early as 36–48 hr after larval hatching (data not presented). Thus, generation of GMCs and differentiated neurons by INPs in *erm¹/erm²* mutant brains is unlikely due to the maternal effect. Alternatively, *erm* may promote GMC differentiation in the type II neuroblast lineage, and in *erm* mutant brains, GMCs might dedifferentiate back into neuroblasts. If so, we would predict an ectopic accumulation of INPs in similarly staged mosaic clones derived from *erm* mutant type II neuroblasts as compared to wild-type clones. However, 48 hr *erm* mutant single neuroblast clones consistently contained fewer INPs when compared to the wild-type clones (Figures 2C–2F). In addition, blocking GMC differentiation by removing Prospero function resulted in ectopic accumulation of INPs but did not lead to ectopic neuroblast formation (Figure 5H). Therefore, the diversity of cells within *erm* mutant clones is also unlikely due to blocking GMC differentiation. We favor the interpretation that *erm* mutant INPs dedifferentiate into apparently normal neuroblasts that can give rise to all cell types found in a type II neuroblast lineage. Consistently, the dedifferentiated neuroblasts in *erm* mutant brains exhibited
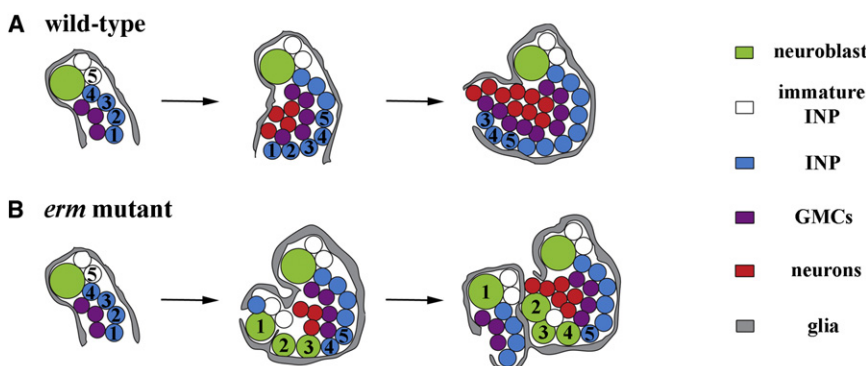

Figure 7. *erm* Maintains the Restricted Developmental Potential of INPs

(A) Wild-type INPs undergo limited rounds of asymmetric divisions to generate neurons prior to exiting from the cell cycle, and they remain in the same glial chamber as their parental type II neuroblasts.

(B) Some *erm* mutant INPs fail to terminate proliferation and dedifferentiate back into their parental type II neuroblast fate. These dedifferentiated neuroblasts can establish ectopic type II neuroblast lineages and form ectopic glial chambers.

normal cortical polarity and proliferation potential (Figures 3 and 4). Furthermore, the dedifferentiated neuroblasts in *erm* mutant brains also lost the expression of *Pros-Gal4* and *Erm-Gal4* and established ectopic type II neuroblast lineages encapsulated by the cortex glial membrane (Figures 3 and 4). Thus, we conclude that Erm likely restricts the developmental potential of INPs by limiting proliferation and suppressing dedifferentiation.

Although mutations in *erm*, *brain tumor*, and *numb* genes all lead to ectopic type II neuroblasts, the proteins appear to regulate INPs at distinct steps in the type II neuroblast lineage (Figure S3). Numb and Brain tumor function cooperatively, but nonredundantly, to ensure that immature INPs undergo maturation and commit to the INP fate (Boone and Doe, 2008; Bowman et al., 2008). While ectopic expression of Numb induces premature differentiation of type II neuroblasts and immature INPs (J. Haenfler, K.L.G., and C.-Y.L., unpublished data), overexpression of Numb is not sufficient to suppress ectopic neuroblasts in *brain tumor* mutant brains (H. Komori and C.-Y.L., unpublished data). Thus, Numb likely promotes differentiation of immature INPs whereas Brain tumor likely prevents immature INPs, which are unstable in nature, from adopting their parental neuroblast fate. More studies will be necessary to discern whether ectopic neuroblasts in *brain tumor* mutant brains arise from dedifferentiation of partially differentiated immature INPs or failure of immature INPs to initiate differentiation. In contrast, immature INPs in *erm* mutant brains mature into functional INPs that exhibit normal cortical polarity and proliferation potential and can generate GMCs and neurons (Figures 2A–2F, 3D, 3E, and 4; Figure S3). Additionally, overexpression of Brain tumor or Numb in INPs was not sufficient to suppress ectopic neuroblasts in *erm* mutant brains (data not shown). Finally, lineage clones derived from single INPs in *erm* mutant brains always contain ectopic type II neuroblasts, multiple immature INPs, INPs, GMCs, and neurons (Figures 3B and 3C). These results indicate that Erm is dispensable for maturation of immature INPs and is not within the genetic hierarchy specifying the INP identity. Instead, Erm maintains the restricted developmental potential of INPs after specification of their identity.

Prospero encodes a homeodomain transcription factor, and nuclear Prospero has been shown to trigger cell cycle exit and GMC differentiation (Choksi et al., 2006; Doe et al., 1991; Maurange et al., 2008). In the wild-type brain, 9.6% of INPs showed nuclear Prospero and were likely undergoing differentiation (data not shown). *prospero* mutant type II neuroblast clones showed ectopic accumulation of INPs but contained single neuroblasts, indicating that blocking differentiation is not sufficient to trigger the dedifferentiation of INPs (Figure 5H). Thus, Prospero restricts the proliferation potential of INPs but does not suppress dedifferentiation of INPs.

While ectopic expression of Prospero in INPs can restore neuronal differentiation in *erm* mutant brains, targeted expression of Erm in neuroblasts or INPs was sufficient to induce rapid nuclear localization of Prospero in these cells and terminate their proliferation (Figure 5). In wild-type brains, Prospero is sequestered in a basal crescent by the adaptor protein Miranda in mitotic neural progenitors (Ikeshima-Kataoka et al., 1997; Shen et al., 1997). Interestingly, mitotic neural progenitors including neuroblasts and INPs transiently overexpressing Erm also showed basal localization and segregation of Miranda and Prospero (data not shown). As such, Erm likely restricts the proliferation potential of INPs by indirectly promoting nuclear localization of Prospero. Therefore, Prospero does not localize in the nuclei of mitotically active INPs, which express Miranda, but does localize in the nuclei of GMCs that do not express Miranda.

How does Erm suppress the dedifferentiation of INPs? Our results show that reduced Notch function can efficiently suppress ectopic neuroblasts in *erm* mutant brains while constitutive activation of Notch signaling induced the dedifferentiation of INPs (Figures 6A–6C). Importantly, coexpression of Erm is sufficient to suppress the dedifferentiation of INPs triggered by expression of constitutively active Notch[intra] (Figure 6D). Together, these results strongly suggest that Erm prevents the dedifferentiation of INPs by antagonizing a Notch-activated mechanism through interfering with the assembly of the Notch transcriptional activator complex or inhibiting the expression of Notch targets. Intriguingly, the amino terminus of all Fezf proteins contains an engrailed homology 1 domain. This domain can mediate direct interaction with the conserved transcriptional corepressor Groucho that can function as a corepressor of Notch signaling (Cinnamon and Paroush, 2008; Copley, 2005; Jeong et al., 2006; Levkowitz et al., 2003; Shimizu and Hibi, 2009). Additional experiments will be needed to discern how Erm antagonizes Notch-activated dedifferentiation of INPs.

EXPERIMENTAL PROCEDURES

Fly Genetics and Transgenes

A total of six *erm* alleles were recovered from EMS mutagenesis following a standard protocol. *erm[2]* was generated by a FRT-based high-resolution deletion method and verified by PCR (Parks et al., 2004). The cDNA for *CG31670* was obtained from the *Drosophila* Genome Resource Center, sequenced, and cloned into the *pUAST-HA* vector for germline transformation. Mouse *fezf1* and *fezf2* cDNAs were sequenced (M. Hibi) and cloned into the *pUAST-HA* vector for germline transformation. *Drosophila* cultures were kept at 25°C on standard cornmeal food. Other mutant alleles and transgenes used in this study include *brat[11]* (Lee et al., 2006c), *pros[17]*, *FRT82B* (Lee et al., 2006c), *aPKC[K06403]* (Lee et al., 2006b), *pins[62]* (Lee et al., 2006b), *UAS-pros* (Hirata et al., 1995), *Wor-gal4* (Lee et al., 2006b), *Ase-gal4* (Zhu et al., 2006), and *R9D-Gal4* lines (Pfeiffer et al., 2008). The *UAS-Notch[RNAi]* lines were obtained from the Vienna *Drosophila* Resource Center. *Oregon R*, *elav-gal4 (C155)*, *hs-flp*, *UAS-mCD8-GFP*, *FRT40A*, *tub-gal80*, *FRT82B*, *hs-flp(F38)*, *act-FRT-Stop-FRT-lacZ*, *UAS-flp*, *tub-GAL80[ts]*, *UAS-dcr-2*, *UAS-Notch[intra]*, *Repo-Gal4* flies were obtained from Bloomington *Drosophila* Stock Center.

Immunofluorescent Staining and Antibodies

Antibody staining was performed as previously described (Lee et al., 2006b). The rabbit Ase antibody was raised against a previously described synthetic peptide (Brand and Perrimon, 1993). Other antibodies used in this study include guinea pig Ase (1:100; J. Knoblich), rat Wor (1:1), rat Dpn (1:1), guinea pig Dpn (1:2500, J. Skeath), mouse Pros (1:100), rat Mira (1:100); guinea pig Mira (1:400), guinea pig Numb (1:3000, J. Skeath); rat Pins (1:500), rabbit Scrib (1:2500), mouse Elav(1:50, DSHB), mouse Dlg (1:100, DSHB), mouse Repo (1:50, DSHB), mouse BrdU (1:50, Roche), rabbit β-gal (1:1000, ICN/Cappel), rat α-Tub (1:100, Sigma), rat mCD8 (1:100, Caltag), rabbit GFP (1:1000, Torreypine), mouse HA (1:1000, Covance), rat HA (1:2000, Roche). Secondary antibodies were from Molecular Probes (details are available upon request). The confocal images were acquired on a Leica SP5 scanning confocal microscope with AOBS.

Edu Pulse-Chase

Larvae were aged for 72 hr after hatching, and were pulse labeled for 3 hr by feeding on the Kankel-White media containing 50 μg/ml EdU (5-ethynyl-2′deoxyuridine) (Lee et al., 2006c). Half of the larvae were processed for staining immediately following the pulse; remaining larvae were transferred to standard media for a 12 hr EdU-free chase. Larvae were dissected and processed for antibody staining as previously described (Lee et al., 2006b). Incorporated EdU was detected by Click-iT fluorescent dye azide reaction as described in the Click-iT product literature (Invitrogen).

Lineage Clonal Analysis

We initially performed genetic clonal analyses of INPs using *Ase-Gal4* by crossing *erm^1, Actin-FRT-Stop-FRT-lacZ/CyO, Actin-GFP* flies to *erm^2, Ase-Gal4/CyO, Actin-GFP; UAS-flp, tub-Gal80^{ts}* flies. At 24 hr after hatching, *erm^1/erm^2* larvae were shifted to 31°C for 48 hr to inactivate Gal80^{ts}, allowing FRT-mediated recombination to induce permanently marked lineage clones. The expression level of *Ase-Gal4* is very low (Bowman et al., 2008), allowing us to induce genetic clones at a very low frequency. However, due to the prolonged incubation time at the nonpermissive temperature, clones derived from two neighboring INPs sometimes became overlapped, resulting in appearance of a "large" clone. We repeated this experiment by using *Erm-Gal4*, whose expression level was significantly higher compared to *Ase-Gal4* (M.W. and C.-Y.L., data not shown). We crossed *erm^1, Actin-FRT-Stop-FRT-lacZ/CyO, Actin-GFP; Erm-Gal4* flies to *erm^2/CyO, Actin-GFP; UAS-flp, tub-Gal80^{ts}* flies. At 24 hr after hatching, *erm^1/erm^2* larvae were shifted to 31°C for 1 hr to induce positively marked genetic clones derived from single INP. Larvae were returned back to 25°C for 72 hr prior to processing larval brains for antibody staining.

Mutant Clonal Analyses

We induced mosaic clones derived from *erm^1* and *pros^{17}* mutant neuroblasts by following a previously established protocol (Lee et al., 2006c; Lee and Luo, 2001).

Overexpression of Notch^{intra}

Overexpression of Notch^{intra} in INPs in larval brains was accomplished by crossing *UAS-Notch^{intra}/CyO, Actin-GFP; tub-Gal80^{ts}* flies to *Erm-Gal4* flies. GFP$^-$ larvae were allowed to hatch at 25°C, and were then shifted to 31°C for 72 hr. Larval brains were dissected and processed for antibody staining. Co-overexpression of Erm and Notch^{intra} was carried out following an identical protocol.

Real-Time PCR

Late third instar larval brains were dissected free of surrounding tissues. Total RNA was extracted following the standard Trizol RNA isolation protocol and cleaned by the QIAGEN RNeasy kit. cDNA was transcribed using First Strand cDNA Synthesis Kit for RT-PCR (AMV) (Roche). Quantitative PCR was performed by using SYBR-green. Resulting data were analyzed by the comparative CT method, and the relative mRNA expression is presented.

SUPPLEMENTAL INFORMATION

Supplemental Information includes three figures and can be found with this article online at doi:10.1016/j.devcel.2009.12.007.

ACKNOWLEDGMENTS

REFERENCES

Bello, B.C., Izergina, N., Caussinus, E., and Reichert, H. (2008). Amplification of neural stem cell proliferation by intermediate progenitor cells in Drosophila brain development. Neural Dev. *3*, 5.

Betschinger, J., Mechtler, K., and Knoblich, J.A. (2006). Asymmetric segregation of the tumor suppressor Brat regulates self-renewal in *Drosophila* neural stem cells. Cell *124*, 1241–1253.

Boone, J.Q., and Doe, C.Q. (2008). Identification of Drosophila type II neuroblast lineages containing transit amplifying ganglion mother cells. Dev. Neurobiol. *68*, 1185–1195.

Bowman, S.K., Rolland, V., Betschinger, J., Kinsey, K.A., Emery, G., and Knoblich, J.A. (2008). The tumor suppressors Brat and Numb regulate transit-amplifying neuroblast lineages in *Drosophila*. Dev. Cell *14*, 535–546.

Brand, A.H., and Perrimon, N. (1993). Targeted gene expression as a means of altering cell fates and generating dominant phenotypes. Development *118*, 401–415.

Chintapalli, V.R., Wang, J., and Dow, J.A.T. (2007). Using FlyAtlas to identify better Drosophila models of human disease. Nat. Genet. *39*, 715–720.

Choksi, S.P., Southall, T.D., Bossing, T., Edoff, K., de Wit, E., Fischer, B.E., van Steensel, B., Micklem, G., and Brand, A.H. (2006). Prospero acts as a binary switch between self-renewal and differentiation in *Drosophila* neural stem cells. Dev. Cell *11*, 775–789.

Cinnamon, E., and Paroush, Z. (2008). Context-dependent regulation of Groucho/TLE-mediated repression. Curr. Opin. Genet. Dev. *18*, 435–440.

Copley, R.R. (2005). The EH1 motif in metazoan transcription factors. BMC Genomics *6*, 169.

Doe, C.Q., Chu-LaGraff, Q., Wright, D.M., and Scott, M.P. (1991). The *prospero* gene specifies cell fates in the *Drosophila* central nervous system. Cell *65*, 451–464.

Farkas, L.M., Haffner, C., Giger, T., Khaitovich, P., Nowick, K., Birchmeier, C., Pääbo, S., and Huttner, W.B. (2008). Insulinoma-associated 1 has a panneurogenic role and promotes the generation and expansion of basal progenitors in the developing mouse neocortex. Neuron *60*, 40–55.

Hashimoto, H., Yabe, T., Hirata, T., Shimizu, T., Bae, Y., Yamanaka, Y., Hirano, T., and Hibi, M. (2000). Expression of the zinc finger gene *fez-like* in zebrafish forebrain. Mech. Dev. *97*, 191–195.

Hirata, J., Nakagoshi, H., Nabeshima, Y., and Matsuzaki, F. (1995). Asymmetric segregation of the homeodomain protein Prospero during Drosophila development. Nature *377*, 627–630.

Hodge, R.D., Kowalczyk, T.D., Wolf, S.A., Encinas, J.M., Rippey, C., Enikolopov, G., Kempermann, G., and Hevner, R.F. (2008). Intermediate progenitors in adult hippocampal neurogenesis: Tbr2 expression and coordinate regulation of neuronal output. J. Neurosci. *28*, 3707–3717.

Ikeshima-Kataoka, H., Skeath, J.B., Nabeshima, Y., Doe, C.Q., and Matsuzaki, F. (1997). Miranda directs Prospero to a daughter cell during Drosophila asymmetric divisions. Nature *390*, 625–629.

Jeong, J.Y., Einhorn, Z., Mercurio, S., Lee, S., Lau, B., Mione, M., Wilson, S.W., and Guo, S. (2006). Neurogenin1 is a determinant of zebrafish basal forebrain dopaminergic neurons and is regulated by the conserved zinc finger protein Tof/Fezl. Proc. Natl. Acad. Sci. USA *103*, 5143–5148.

Lee, T., and Luo, L. (2001). Mosaic analysis with a repressible cell marker (MARCM) for Drosophila neural development. Trends Neurosci. *24*, 251–254.

Lee, C.-Y., Andersen, R.O., Cabernard, C., Manning, L., Tran, K.D., Lanskey, M.J., Bashirullah, A., and Doe, C.Q. (2006a). Drosophila Aurora-A kinase

inhibits neuroblast self-renewal by regulating aPKC/Numb cortical polarity and spindle orientation. Genes Dev. *20*, 3464–3474.

Lee, C.Y., Robinson, K.J., and Doe, C.Q. (2006b). Lgl, Pins and aPKC regulate neuroblast self-renewal versus differentiation. Nature *439*, 594–598.

Lee, C.Y., Wilkinson, B.D., Siegrist, S.E., Wharton, R.P., and Doe, C.Q. (2006c). Brat is a Miranda cargo protein that promotes neuronal differentiation and inhibits neuroblast self-renewal. Dev. Cell *10*, 441–449.

Levkowitz, G., Zeller, J., Sirotkin, H.I., French, D., Schilbach, S., Hashimoto, H., Hibi, M., Talbot, W.S., and Rosenthal, A. (2003). Zinc finger protein too few controls the development of monoaminergic neurons. Nat. Neurosci. *6*, 28–33.

Matsuo-Takasaki, M., Lim, J.H., Beanan, M.J., Sato, S.M., and Sargent, T.D. (2000). Cloning and expression of a novel zinc finger gene, Fez, transcribed in the forebrain of Xenopus and mouse embryos. Mech. Dev. *93*, 201–204.

Maurange, C., Cheng, L., and Gould, A.P. (2008). Temporal transcription factors and their targets schedule the end of neural proliferation in *Drosophila*. Cell *133*, 891–902.

Morrison, S.J., and Kimble, J. (2006). Asymmetric and symmetric stem-cell divisions in development and cancer. Nature *441*, 1068–1074.

Parks, A.L., Cook, K.R., Belvin, M., Dompe, N.A., Fawcett, R., Huppert, K., Tan, L.R., Winter, C.G., Bogart, K.P., Deal, J.E., et al. (2004). Systematic generation of high-resolution deletion coverage of the Drosophila melanogaster genome. Nat. Genet. *36*, 288–292.

Pereanu, W., Shy, D., and Hartenstein, V. (2005). Morphogenesis and proliferation of the larval brain glia in Drosophila. Dev. Biol. *283*, 191–203.

Pfeiffer, B.D., Jenett, A., Hammonds, A.S., Ngo, T.T., Misra, S., Murphy, C., Scully, A., Carlson, J.W., Wan, K.H., Laverty, T.R., et al. (2008). Tools for neuro-anatomy and neurogenetics in Drosophila. Proc. Natl. Acad. Sci. USA *105*, 9715–9720.

Pontious, A., Kowalczyk, T., Englund, C., and Hevner, R.F. (2008). Role of intermediate progenitor cells in cerebral cortex development. Dev. Neurosci. *30*, 24–32.

Sessa, A., Mao, C.A., Hadjantonakis, A.K., Klein, W.H., and Broccoli, V. (2008). Tbr2 directs conversion of radial glia into basal precursors and guides neuronal amplification by indirect neurogenesis in the developing neocortex. Neuron *60*, 56–69.

Shen, C.P., Jan, L.Y., and Jan, Y.N. (1997). Miranda is required for the asymmetric localization of Prospero during mitosis in Drosophila. Cell *90*, 449–458.

Shimizu, T., and Hibi, M. (2009). Formation and patterning of the forebrain and olfactory system by zinc-finger genes Fezf1 and Fezf2. Dev. Growth Differ. *51*, 221–231.

Vescovi, A.L., Galli, R., and Reynolds, B.A. (2006). Brain tumour stem cells. Nat. Rev. Cancer *6*, 425–436.

Wang, H., Somers, G.W., Bashirullah, A., Heberlein, U., Yu, F., and Chia, W. (2006). Aurora-A acts as a tumor suppressor and regulates self-renewal of Drosophila neuroblasts. Genes Dev. *20*, 3453–3463.

Zhu, S., Lin, S., Kao, C.F., Awasaki, T., Chiang, A.S., and Lee, T. (2006). Gradients of the *Drosophila* Chinmo BTB-zinc finger protein govern neuronal temporal identity. Cell *127*, 409–422.